



Since January 2020 Elsevier has created a COVID-19 resource centre with free information in English and Mandarin on the novel coronavirus COVID-19. The COVID-19 resource centre is hosted on Elsevier Connect, the company's public news and information website.

Elsevier hereby grants permission to make all its COVID-19-related research that is available on the COVID-19 resource centre - including this research content - immediately available in PubMed Central and other publicly funded repositories, such as the WHO COVID database with rights for unrestricted research re-use and analyses in any form or by any means with acknowledgement of the original source. These permissions are granted for free by Elsevier for as long as the COVID-19 resource centre remains active.



Contents lists available at ScienceDirect

Journal of Integrative Medicine

journal homepage: www.jcimjournal.com/jim
www.journals.elsevier.com/journal-of-integrative-medicine

Original Research Article

Active constituents and mechanisms of Respiratory Detox Shot, a traditional Chinese medicine prescription, for COVID-19 control and prevention: Network-molecular docking-LC-MS^E analysisZi-jia Zhang^{a,1}, Wen-yong Wu^{a,b,1}, Jin-jun Hou^{a,1}, Lin-lin Zhang^a, Fei-fei Li^{a,b}, Lei Gao^{a,b}, Xing-dong Wu^a, Jing-ying Shi^{a,b}, Rong Zhang^{a,b}, Hua-li Long^a, Min Lei^a, Wan-ying Wu^{a,*}, De-an Guo^{a,*}, Kai-xian Chen^{a,*}, Lewis A. Hofmann^c, Zhong-hua Ci^c^a Shanghai Institute of Materia Medica, Chinese Academy of Sciences, Shanghai 201203, China^b University of Chinese Academy of Sciences, Beijing 100049, China^c World Health Science Organization, Leesburg, VA 20176, USA

ARTICLE INFO

Article history:

Received 13 March 2020

Accepted 17 March 2020

Available online 8 April 2020

Keywords:

Lung-toxin Dispelling Formula No. 1
COVID-19
3C-like protease
Network pharmacology
Molecular docking
Meridian tropism

ABSTRACT

Objective: Lung-toxin Dispelling Formula No. 1, referred to as Respiratory Detox Shot (RDS), was developed based on a classical prescription of traditional Chinese medicine (TCM) and the theoretical understanding of herbal properties within TCM. Therapeutic benefits of using RDS for both disease control and prevention, in the effort to contain the coronavirus disease 2019 (COVID-19), have been shown. However, the biochemically active constituents of RDS and their mechanisms of action are still unclear. The goal of the present study is to clarify the material foundation and action mechanism of RDS.

Methods: To conduct an analysis of RDS, an integrative analytical platform was constructed, including target prediction, protein-protein interaction (PPI) network, and cluster analysis; further, the hub genes involved in the disease-related pathways were identified, and their corresponding compounds were used for *in vitro* validation of molecular docking predictions. The presence of these validated compounds was also measured in samples of the RDS formula to quantify the abundance of the biochemically active constituents. In our network pharmacological study, a total of 26 bioinformatic programs and databases were used, and six networks, covering the entire Zang-fu viscera, were constructed to comprehensively analyze the intricate connections among the compounds-targets-disease pathways-meridians of RDS.

Results: For all 1071 known chemical constituents of the nine ingredients in RDS, identified from established TCM databases, 157 passed drug-likeness screening and led to 339 predicted targets in the constituent-target network. Forty-two hub genes with core regulatory effects were extracted from the PPI network, and 134 compounds and 29 crucial disease pathways were implicated in the target-constituent-disease network. Twelve disease pathways attributed to the Lung-Large Intestine meridians, with six and five attributed to the Kidney-Urinary Bladder and Stomach-Spleen meridians, respectively. One-hundred and eighteen candidate constituents showed a high binding affinity with SARS-coronavirus-2 3-chymotrypsin-like protease (3CL^{PRO}), as indicated by molecular docking using computational pattern recognition. The *in vitro* activity of 22 chemical constituents of RDS was validated using the 3CL^{PRO} inhibition assay. Finally, using liquid chromatography mass spectrometry in data-independent analysis mode, the presence of seven out of these 22 constituents was confirmed and validated in an aqueous decoction of RDS, using reference standards in both non-targeted and targeted approaches.

Conclusion: RDS acts primarily in the Lung-Large Intestine, Kidney-Urinary Bladder and Stomach-Spleen meridians, with other Zang-fu viscera strategically covered by all nine ingredients. In the context of TCM meridian theory, the multiple components and targets of RDS contribute to RDS's dual effects of health-strengthening and pathogen-eliminating. This results in general therapeutic effects for early COVID-19 control and prevention.

* Corresponding authors.

E-mail addresses: wanyingwu@simm.ac.cn (W.Y. Wu), daguo@simm.ac.cn (D.A. Guo), kxchen@simm.ac.cn (K.X. Chen).¹ These authors made equal contribution to this work.<https://doi.org/10.1016/j.joim.2020.03.004>

2095-4964/© 2020 Shanghai Changhai Hospital. Published by Elsevier B.V. All rights reserved.

Please cite this article as: Zhang ZJ, Wu WY, Hou JJ, Zhang LL, Li FF, Gao L, Wu XD, Shi JY, Zhang R, Long HL, Lei M, Wu WY, Guo DA, Chen KX, Hofmann LA, Ci ZH. Active constituents and mechanisms of Respiratory Detox Shot, a traditional Chinese medicine prescription, for COVID-19 control and prevention: Network-molecular docking-LC-MS^E analysis. *J Integr Med.* 2020; 18(3): 229–241.

© 2020 Shanghai Changhai Hospital. Published by Elsevier B.V. All rights reserved.

1. Introduction

On January 30, 2020, the World Health Organization (WHO) announced that the outbreak of new coronavirus disease (coronavirus disease 2019 [COVID-19]) was a public health emergency of international concern (PHEIC) [1,2]. It is the 6th time the WHO has declared a PHEIC since the International Health Regulations came into effect in 2005 [2,3]. COVID-19 has spread to nearly 90 countries, with more than one hundred thousand confirmed cases, endangering the health of people all over the world and causing a global health crisis [4,5].

In the recent effort to contain COVID-19, effective preparedness and response have been made for the prevention and control of the disease in China, and the preliminary results have been promising [5,6]. However, no effective treatment for infected patients with COVID-19 has been identified or approved as of the writing of this report.

From the perspective of traditional Chinese medicine (TCM), COVID-19 can be considered a “plague.” TCM has played an essential role in prevention and control of plagues in China. Throughout the history of combating plagues, TCM has gradually forged a unique and complete system with invaluable experience in both theoretical and practical levels of treatment. In recent history, TCM has provided alternative treatments for the effective prevention and control of novel acute respiratory tract infections around the world [7,8]. Presently, the integration of TCM and allopathic medicine has formed the dominant treatment strategy in all COVID-19-affected areas across China [9].

The Lung-toxin Dispelling Formula No. 1 (祛肺毒一号方), referred to as Respiratory Detox Shot (RDS), is based on the theory of TCM medicinal properties, the classical prescription of TCM and clinical practice. There are nine TCM ingredients in RDS: Schizonepetae Herba (Jingjie), Lonicerae Japonicae Flos (Jinyinhua), Forsythiae Fructus (Lianqiao), Scrophulariae Radix (Xuanshen), Gleditsiae Spina (Zaojiaoci), Armeniacae Semen Amarum (Kuxingren), Nidus Vespae (Fengfang), Glycyrrhizae Radix et Rhizoma (Gancao) and Ginseng Radix et Rhizoma (Renshen). The nine TCM ingredients in this prescription have been used together as an herbal formula in clinical practice for more than a decade and have been effective for the prevention and treatment of acute respiratory tract infections, as well as the common cold and flu. In recent months, clinical trials of RDS have been conducted to evaluate its efficacy in patients with severe/critical COVID-19 pneumonia, finding that RDS has treatment value and no observed side effects [10]. Additionally, eight out of the nine ingredients in RDS are plant-derived; the other ingredient is honeycomb. All nine ingredients are approved as dietary supplements by the United States Food and Drug Administration, indicating that their long-term use is considered to be safe in the US. RDS has therapeutic benefits in both disease prevention and treatment against COVID-19; these benefits may have global significance [10].

TCM has substantial advantages in treating complicated and severe diseases and has strong clinical support, but it is still considered as an alternative or complementary medicine, mainly because of that the specific biochemically active constituents of its prescriptions or their mechanisms of action are not identified. The critical problem of the COVID-19 pandemic demands novel

strategies that reach beyond conventional antiviral treatments [8,11–13]. To better understand and promote the clinical use of RDS globally, this study investigates important biochemical constituents present in the formula and the biological processes that they may effect, eliciting the therapeutic effects of RDS.

Even though technological limitations in drug research have been reduced over time, challenges still exist in studying the biochemically active constituents present in TCM prescriptions and their mechanisms of action. TCM prescriptions present a complex chemical system, comprised of multiple TCM herbs. The complex nature of TCM makes it difficult to study the action of the full prescription through the reductionist approach taken in contemporary medical research, which would recommend separating out individual herbal ingredients and potential targets in the investigation process [14,15]. In the era of -omics technologies, a vast amount of data have become available and in some avenues of research, the focus has shifted emphasis from the classic “drug-reductionist” to the novel “drug-holistic” system-based approaches [16]. Network pharmacology is a branch of systems biology, which explores the correlation between drugs and diseases from a comprehensive perspective; this is consistent with the holistic view, systematic approach and compatibility principle of TCM [17–19].

The structure of 3-chymotrypsin-like protease (3CL^{pro}) was determined after the emergence of severe acute respiratory syndrome (SARS) [20,21]. It is the main protease that cleaves host polyproteins into viral replication-related proteins, and is highly conserved across the coronavirus family, including SARS coronavirus 2 (SARS-CoV-2), SARS coronavirus (SARS-CoV) and Middle East respiratory syndrome coronavirus [22]. Therefore, it is an important target for the design of potential anti-coronavirus inhibitors [23]. One efficient approach used to screen potential active compounds against specific target proteins, such as 3CL^{pro}, is molecular docking simulation [22–25]. It is a universal and efficient approach in modern drug design and drug discovery.

The present study is designed based on the success of network analysis. A network of interactions among each TCM in the RDS formula, their meridian tropism, chemical composition and potential target proteins was established to investigate the possible pathways of action. This approach helps to predict the biochemically active constituents of this TCM prescription; it also provides a way to develop an in-depth understanding of how a complex drug system works to treat a complex disease. It is an important research strategy to understand the possible intervention mechanism of RDS on COVID-19 from the perspective of the biological and molecular networks. This knowledge could help to develop an early prevention and treatment scheme to manage COVID-19 pneumonia. In this study, the ability of the active constituents of RDS to bind with SARS-CoV-2 3CL^{pro} (6LU7) was evaluated using computational pattern recognition to test the likelihood of molecular docking. Finally, the chemical constituents present in RDS were tested against the putative biochemically active constituents identified in this study using ultrahigh-performance liquid chromatography (UPLC), coupled with tandem mass spectrometry in data-independent analysis mode (MS^E) with non-targeted and targeted approaches. Through the above studies, biochemically active constituents from the RDS formula and their likely pathways of action were identified.

2. Materials and methods

Version, accession information and web addresses of the databases and software are listed in the online supplementary Table S1. Due to the differences in data entry format across databases and platforms, we use HUGO Gene Nomenclature Committee (HGNC) gene symbol format to present the genes in our study to avoid confusion or incompatibility in data processing [26].

2.1. Network pharmacology

2.1.1. Construction of the ingredient–property–flavor–meridian tropism network for RDS prescription

There are nine ingredients in the RDS prescription, and the corresponding information about their TCM properties (hot, cold, warm, cool and neutral), flavors (sweet, bitter, pungent and salty) and meridian tropisms (Lung, Stomach, Heart, Spleen, Liver, Kidney, Large Intestine and Small Intestine) were compiled from the 2015 *Chinese Pharmacopoeia*, Encyclopedia of Traditional Chinese Medicine (ETCM), Symptom Mapping (SymMap), Natural Product Activity and Species Source Database (NPASS) and Traditional Chinese Medicines Integrated Database (TCMID; Table S1) [27–32]. A network of ingredient–property–flavor–meridian tropism was constructed using Cytoscape 3.7.2 [33]. Connection degree was calculated by Cytoscape as a measure of the number of “in” and “out” links one node has to other nodes.

2.1.2. Chemical constituent database construction, target prediction and target gene retrieval

Chemical constituents contained in each of the nine ingredients of the RDS prescription were obtained from two TCM databases: Traditional Chinese Medicine Systems Pharmacology (TCMSP, <http://www.tcmspw.com/tcmsp.php>) or TCMID (<http://119.3.41.228:8000/tcmid/>) [30,31]. The predicted targets of these constituents were acquired from the TCMSP database by setting the built-in drug-likeness screening criteria as oral bioavailability $\geq 30\%$ and drug-likeness ≥ 0.18 . Constituents identified from the TCMID database were first applied to the FAFDrugs4 platform, an external drug-likeness screening database, and only compounds passing the Drug-like soft filters were kept for the next stage of target prediction [34]. Information on individual chemical constituents was further processed with SEA, TargetNet and SwissTargetPrediction databases to further describe their predicted targets, as described in our earlier study [19,35–37]. Targets predicted using the above two strategies were pooled, and detailed information about the genes corresponding to the predicted targets was queried using UniProt, GeneCards and STRING databases [38–40].

2.1.3. Construction of the RDS network

Cytoscape 3.7.2 software was used to construct the network and conduct topological analysis [33]. The binary high-quality interactome of *Homo sapiens* (62435 queries, on 03/04/2020) was downloaded from the High-quality INTERactomes (HINT) database, which curates a compilation of high-quality protein–protein interactions from eight interactome resources [41]. All the downloaded queries were processed by Cytoscape, and an HINT network was constructed as an initial framework, using the method described by Zhao et al. [42]. Then, the RDS targets, identified above, were mapped onto the HINT network and this system was referred to as the RDS network.

2.1.4. Submodule recognition and protein–protein interaction analysis of the RDS network and the KEGG biological pathway enrichment

To better understand the RDS network, submodules of the network were clustered using the MCODE plug-in for Cytoscape

[19,33,43]. Each submodule represents a group of genes that require tight mutual regulation to achieve their molecular functions. The default settings of the MCODE plug-in were adopted as follows: Network Scoring–Include Loops: false; Degree Cutoff: 2; Cluster Finding–Node Score Cutoff: 0.2; Haircut: true; Fluff: false; K-Core: 2; Max. Depth from Seed: 100. The biological pathways involved in the submodules were further analyzed. To explore the structural and functional connections of the genes in the submodules, enrichment analysis of “protein complex-based gene sets” was performed using the ConsensusPathDB (CPDB) database [44,45].

2.1.5. Construction of the RDS hub gene network and evaluation of RDS regulatory strength on the targets

To further focus on the more important genes among the 148 targets in the RDS network, the RDS hub gene network was constructed by selecting the corresponding nodes and edges with the highest degree of connection. In the RDS network, nodes with the highest connection score were defined as “RDS hub genes.”

To evaluate the strength of individual constituents in the RDS prescription on the RDS hub gene network, we introduced a parameter called target “regulated strength score (RSS),” which was defined as follows:

$$RSS = \sum_{i=1}^n C_i$$

where n is the total number of chemical constituents that target each RDS hub gene and $C_1 (C_2, C_3, \dots, C_n)$ is the number of ingredients in the RDS formula that contain that constituent.

The higher the RSS, the stronger the effect compounds in the prescription are on the targets.

2.1.6. Target–pathway and disease–target construction with DAVID and STRING databases

The RDS hub genes were analyzed with the STRING database for KEGG pathway enrichment analysis within the scope of human disease, and the false discovery rate (FDR) was set below 1×10^{-6} [40].

Analyses were performed on RDS hub genes using both STRING and DAVID databases for disease-related pathways. For the DAVID database, “functional annotation clustering” was chosen under disease analysis [40,46], and the “Classification stringency” was set at high, prior to discovering disease pathways. The disease-related pathways from both databases were combined, and entries with non-specific disease pathways were manually removed. Viral infection-related disease pathways were listed in their own group, and other disease pathways were further classified based on their affected meridians in TCM Zang-fu viscera theory.

An integrative network was constructed based on the disease pathways, their corresponding meridian tropism, RDS hub genes, corresponding chemical constituents and TCM ingredients.

2.2. Molecular docking of RDS chemical constituents with SARS-CoV-2 3CL^{pro} (6LU7)

The three dimensional (3D) structures of the chemical constituents of RDS were first constructed with ChemOffice software and saved in mol2 format; their energies were minimized under a MMFF94 force field. The 3D structure of 3CL^{pro} was downloaded from the RCSB Protein Data Bank (PDB) in PDB format [47,48]. PyMOL software was used for protein dehydrating, hydrogenation and other operations, while the AutoDock software was used to convert the compounds and target protein format to PDBQT format [49]. Finally, AutoDock Vina was run for virtual docking [50]. A binding energy less than zero indicates that a ligand can

spontaneously bind to the receptor. It is generally accepted that when the conformation of ligand and receptor binding is stable, the lower the energy is, the more likely the binding is to occur. The binding energy ≤ -5.0 kJ/mol was selected as the screening criteria.

2.3. Analysis of chemical material basis of RDS

2.3.1. Reagents and materials

High-performance liquid chromatography grade methanol and gradient grade acetonitrile were obtained from Fisher Scientific (Ottawa, Canada) and Merck KGaA (Darmstadt, Germany), respectively. Liquid chromatography–mass spectrometry (LC–MS) grade ammonium formate was purchased from Fluka (Buchs, Switzerland), and formic acid 98%–100% from Merck KGaA was used to prepare the mobile phase. Type-1 water (18.2 M Ω .cm) was obtained from Milli-Q Biocel (Millipore, Billerica, MA, USA). All chemical standards were purchased from Shanghai Standard Technology Co., Ltd. and Chengdu DeSiTe Biological Technology Co., Ltd.

Each of the nine herbs and the decoction of RDS were provided by Shanghai Cai Tong De Pharmacy, China.

2.3.2. Sample preparation and solutions

Dried powder (0.3 g) from an RDS decoction was placed in a 50 mL centrifuge tube, soaked and ultrasonically solubilized in 25 mL of 50% methanol (v/v) for 30 min. After centrifugation at 11,000 r/min for 10 min, the supernatant was used in further analysis. Each of the herbs was also extracted separately in water and dried under vacuum. A 0.1 g sample of the dried powder from each extract was solubilized following the above method.

For identification, the stock solution of each chemical standard was prepared in methanol, and two mixed standard solutions were diluted with 50% methanol (v/v) to about 20 μ g/mL.

2.3.3. UPLC/quadrupole time-of-flight MS^E conditions

The LC–MS analysis was performed on a Waters ACQUITY I-Class UPLC (Waters, Milford, MA, USA), equipped with a binary solvent manager, a sample manager and a column manager. A Waters HSS T3 column (2.1 mm \times 150 mm, 1.7 μ m) was equipped together with a Waters in-line filter. Samples were run at 35 $^{\circ}$ C. The mobile phase consisted of acetonitrile containing 0.1% formic acid (v/v) (B) and water containing 0.1% formic acid (v/v) (A). The following gradient elution program was used: 0–2 min, 0–2% (B); 2–22 min, 2%–60% (B); 22–24 min, 60%–90% (B); 24–29 min, 90% (B); 29–30 min, 90%–100% (B); 30–35 min, 100% (B); 35–36 min, 100%–0% (B); 36–41 min, 0% (B). Post-column infusion was performed with methanol containing 10 mmol/L ammonium formate and 0.05% formic acid (0.2 mL/min). The flow rate was set at 0.4 mL/min. A 2 μ L aliquot of each test solution was injected for UPLC analysis.

High-accuracy mass spectrometric data were recorded on a Waters Xevo G2-S QTOF mass spectrometer (Waters, Manchester, UK). Tune parameters were set for LC–MS in data-independent analysis mode (LC–MS^E): capillary voltage was 2.5 kV (negative mode) and 3.0 kV (positive mode); sampling cone was 40 V; source offset voltage was 60 V; source temperature was 150 $^{\circ}$ C; desolvation temperature was 500 $^{\circ}$ C; cone gas flow was 20 L/h and desolvation gas was 800 L/h. The mass analyzer scanned over a mass range of 50–1200 D within 0.1 s under low collision energy at 6 V. A high collision energy ramp of 15–60 V for negative mode and positive mode was employed. Data calibration was performed using an external reference (LockSprayTM) infused with 1 ng/ μ L of leucine enkephalin (Sigma-Aldrich, St. Louis, MO, USA) at a flow rate of 5 μ L/min and with reference to the ion m/z 554.2620 for negative and 556.2766 for positive. Data acquisition was controlled by MassLynx V4.1 software (Waters Corporation,

Milford, USA). Automatic metabolite characterization was performed using UNIFI 1.9.4 (Waters, Milford, USA) through the search of in-house library.

3. Results

3.1. Network pharmacological results

3.1.1. The ingredient–property–flavor–meridian tropism network for RDS prescription

Based on TCM theory, the nine ingredients in RDS were classified by their property, flavor and meridian tropism (Fig. 1 and Table 1). A network was constructed among elements of the TCM classification system (Table 1) and the nine ingredients of the RDS prescription, using the Cytoscape software (Fig. 1). The three nodes with the highest degree of connection in the network are Lung, Stomach and Heart, with corresponding connection values of seven, five and four, respectively. Seven ingredients in RDS are associated with the Lung meridian; Gleditsiae Spina and Nidus Vespae are the exceptions. Among the flavor nodes, the three with the greatest degree of connection are sweet, bitter and warm; their connection degrees in the network are five, four and four, respectively.

3.1.2. Chemical constituent database construction, target prediction and target gene retrieval

Among the nine herbs of the RDS prescription, eight were documented in the TCMSD database. The remaining one, Nidus Vespae, was found in the TCMID database. Information on the

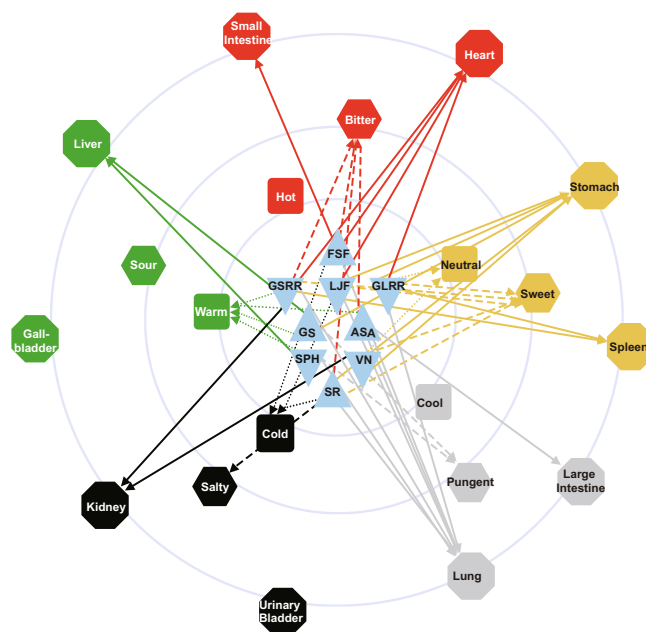


Fig. 1. The ingredient–property–flavor–meridian tropism network of the RDS prescription. The network shows the interconnection of the nine ingredients in RDS and corresponding information about their TCM properties (hot, cool, warm, cold and neutral), flavors (sour, bitter, sweet, pungent and salty) and meridian tropisms (Liver, Gallbladder, Heart, Small Intestine, Spleen, Stomach, Lung, Large Intestine, Kidney and Urinary Bladder). The color scheme of the nodes and edges corresponds with the five elements and colors in TCM theory: green, wood; red, fire; yellow, earth; white, gold; black, water. Blue: the nine ingredients in RDS. ASA: *Armeniacae Semen Amarum* (Kuxingren); FSF: *Forsythiae Fructus* (Lianqiao); GLRR: *Glycyrrhizae Radix et Rhizoma* (Gancao); GS: *Gleditsiae Spina* (Zaojiaoqi); GSR: *Ginseng Radix et Rhizoma* (Renshen); LJJ: *Lonicerae Japonicae Flos* (Jinyinhua); RDS: *Respiratory Detox Shot*; SPH: *Schizonepetae Herba* (Jingjie); SR: *Scrophulariae Radix* (Xuanshen); TCM: traditional Chinese medicine; VN: *Nidus Vespae* (Fengfang).

Table 1
Property, flavor and meridian tropism of ingredients in Respiratory Detox Shot.

Ingredient	Property			Flavor				Meridian tropism							
	Warm	Cold	Neutral	Sweet	Bitter	Pungent	Salty	Lung	Stomach	Heart	Spleen	Liver	Kidney	Large Intestine	Small Intestine
Ginseng Radix et Rhizoma	✓			✓	✓			✓		✓	✓		✓		
Glycyrrhizae Radix et Rhizoma			✓	✓				✓	✓	✓					
Schizonetepetae Herba	✓					✓		✓							
Lonicerae Japonicae Flos		✓		✓				✓							
Armeniaca Semen Amarum	✓				✓			✓							
Forsythiae Fructus		✓			✓			✓							
Scrophulariae Radix	✓			✓	✓			✓					✓		✓
Gleditsiae Spina						✓						✓			
Nidus Vespae			✓	✓											
Total	4	3	2	5	4	2	1	7	5	4	2	2	2	1	1

✓: Ingredient in Respiratory Detox Shot with the identified poverty, flavor and meridian tropism.

chemical constituents contained in individual ingredients of the RDS prescription was also found in the TCMSP and TCMID databases. A total of 1071 constituents were retrieved for all nine herbs. A total of 157 of these constituents passed the drug-likeness screening, and 339 preliminary targets were obtained in the target identification process (Table S2). The chemical constituents, their targets and their presence in RDS ingredients are reported in Fig. S1. The constituents that present among more than one ingredient are also identified in Table S3.

3.1.3. Construction of RDS ingredient–constituent–target and protein–protein interaction networks

Preliminary targets (339) of RDS constituents were mapped onto a HINT network, and the results were filtered, resulting in a reduced network with 346 edges and 148 nodes (i.e., 148 targets). This is referred to as the RDS network. These 148 targets corresponded to 155 chemical constituents; their connection with the ingredients of RDS is shown in Fig. 2. The protein–protein interactions were analyzed to reveal interactions among 148 target genes in the RDS network (Fig. 3).

3.1.4. Submodule analysis and protein–complex recognition of RDS target network with KEGG biological pathway enrichment

To find the clusters in the RDS network, submodule recognition analysis was performed on the 148 targets of the RDS network. Six submodules were identified, covering 23 out of the 148 targets (Fig. 4). Gene ontology analysis via STRING revealed that 19 of the 23 genes were related to nucleoplasm.

To further reveal the structural and functional connections of the 23 genes in the submodules, enrichment analysis of “protein complex-based gene sets” was performed using the CPDB database. The results showed that gene products in Submodule 4 can form the “integrin α 4 β 1:vascular cell adhesion molecule-1 (VCAM-1)” protein complex (complex source: reactome; P value = 1.15×10^{-8} ; Fig. 4d). Further, Submodule 3 can form an inhibitor of κ B (I κ B) kinase complex, including I κ B kinase (IKK), inhibitor of nuclear factor κ B kinase subunit α (IKKA, CHUK), elongator complex protein 1 (ELP1, IKBKAP), nuclear factor κ B inhibitor α (NFKBIA), transcription factor p65 (NFKB3, RELA) and mitogen-activated protein kinase 14 (MAP3K14; complex source: CORUM; P value = 2.28×10^{-7} ; Fig. 4c). Additionally, cyclin-dependent kinase 4 and 6 (CDK4 and CDK6) and cyclin D2 (CCND2) in Submodule 5 can also form a protein complex (Fig. 4e).

3.1.5. Construction of RDS hub gene network and evaluation of RDS regulatory strength on the network

To further scrutinize the more important genes among the 148 targets in the RDS network, topological analysis was performed to calculate the average connection of the network. The mean node degree is 4.7, and the median is three. Therefore, nodes with a node degree greater than or equal to six are considered hub nodes, or the hub genes of the network. Forty-two hub genes were identified in the RDS target network (Fig. 3).

To measure the strength of regulatory effects on hub genes, we introduced a parameter called “RSS.” Among the 42 hub genes of the target network, 11 genes had an RSS higher than 30.

3.1.6. Target–pathway and disease–target network construction with DAVID and STRING databases

The 42 hub gene proteins were uploaded to the STRING database for functional enrichment analysis. The statistical indicator was set as $FDR < 1 \times 10^{-6}$. Thirty-nine pathways were obtained from the pathway enrichment analysis, and the top entries were signal transduction, transport and catabolism, cell growth and death, cellular community–eukaryotes, immune system, neural system, nervous system, development and regeneration (Fig. 5).

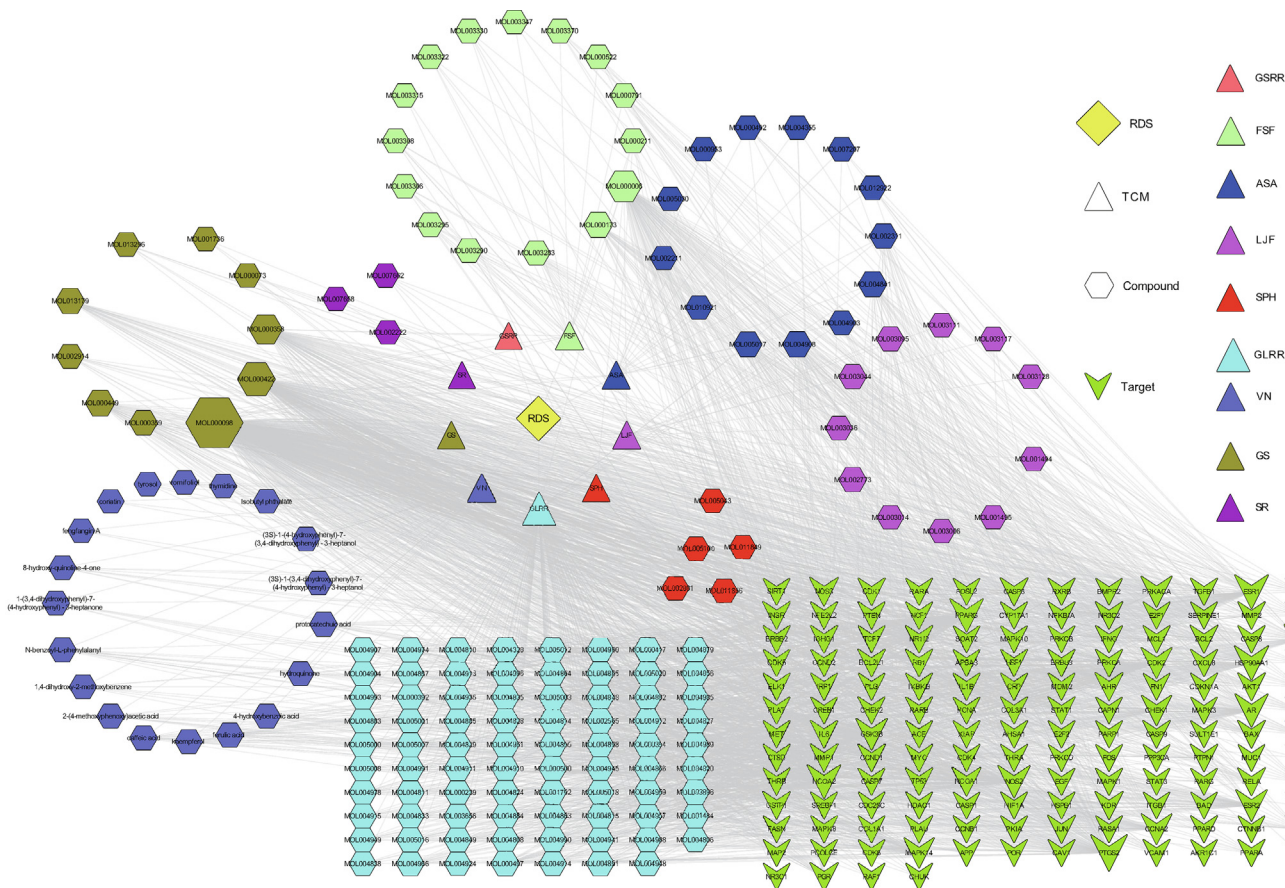


Fig. 2. RDS ingredient-constituent-target network. After mapping onto the HINT background network, the RDS network showed interconnections among the 148 predicted targets of RDS, the corresponding 155 constituents, and the nine ingredients. Diamond, RDS prescription; triangles, TCM ingredients in RDS; hexagons, chemical constituents TCM ingredients; arrowhead, predicted targets of RDS. ASA: Armeniacae Semen Amarum (Kuxingren); FSF: Forsythiae Fructus (Lianqiao); GLRR: Glycyrrhizae Radix et Rhizoma (Gancao); GS: Gleditsiae Spina (Zaojiaoci); GSRR: Ginseng Radix et Rhizoma (Renshen); HINT: High-quality INTERactomes; LJF: Lonicerae Japonicae Flos (Jinyinhua); RDS: Respiratory Detox Shot; SPH: Schizonepetae Herba (Jingjie); SR: Scrophulariae Radix (Xuanshen); TCM: traditional Chinese medicine; VN: Nidus Vespa (Fengfang).

Enrichment analysis of the 42 hub genes via STRING and DAVID databases identified 29 related diseases, which involve 38 targets, corresponding to 134 chemical constituents of the nine ingredients comprising the RDS formula (Fig. 6). Among them, 12 diseases were attributed to the Lung and Large Intestine meridians; they involved 32 targets that were related to 118 of the chemical constituents present in RDS. There were 4 disease pathways attributed to Liver and Gallbladder meridians, involving 18 targets that were related to 92 constituents. There were 6 disease pathways attributed to Kidney and Urinary Bladder meridians, involving 29 targets that were related to 125 constituents. There were 5 disease pathways attributed to Stomach and Spleen meridians, involving 14 targets that were related to 115 constituents, and 2 diseases attributed to Heart and Small Intestine meridians, involving 5 targets that were related to 121 constituents.

Further, the disease-target network analysis revealed that there were seven pathways related to viral infections in the enrichment analysis (Fig. S2).

Based on the disease-targets-compounds network, five most connected compounds were MOL000098, MOL000006, MOL000173, MOL000497 and MOL000422, with connection degrees of 26, 19, 17, 16 and 16, respectively. The five most connected genes were estrogen receptor 1 (*ESR1*), heat-shock protein 90 kDa α (cytosolic) class A member 1 (*HSP90AA1*), androgen receptor (*AR*), peroxisome proliferator-activated receptor γ (*PPARG*), and glycogen synthase kinase 3 β (*GSK3B*), which had

connection degrees of 106, 90, 88, 85 and 75, respectively; this finding was in agreement with the protein-protein interaction analysis shown in Fig. 3.

There are five ingredients in the RDS formula that exert effects on the Stomach meridian, two ingredients on the Spleen meridian and two ingredients on the Kidney meridian. The Stomach, Spleen, and Kidneys are the Zang-fu viscera considered by TCM theory to generate the postnatal and prenatal Qi, which together determine one's overall wellness. Four ingredients in the RDS formula exert effects on the Heart meridian, and help to counteract the Lung's potential excessive reaction to the disease. Two ingredients exert a regulatory effect on the Liver, prevent the Liver from overcontrolling the Lung, and thus allow the Lung full ability to respond to and fight the disease. From the TCM property and flavor perspectives, there are 4 warm, 3 cool and 2 neutral ingredients; 5 of the ingredients are sweet, 4 bitter, 2 pungent, and one has a salty flavor.

3.2. Molecular docking with SARS-CoV-2 3CL^{pro} (6LU7) and antiviral potential of RDS

To find out if RDS compounds will interact directly with SARS-CoV-2, molecular docking was modeled to evaluate the binding affinity between chemical constituents of RDS and 3CL^{pro} (Fig. 7). After preliminary screening, the binding affinity between 118 constituents of RDS and 3CL^{pro} was calculated, alongside 14 antiviral

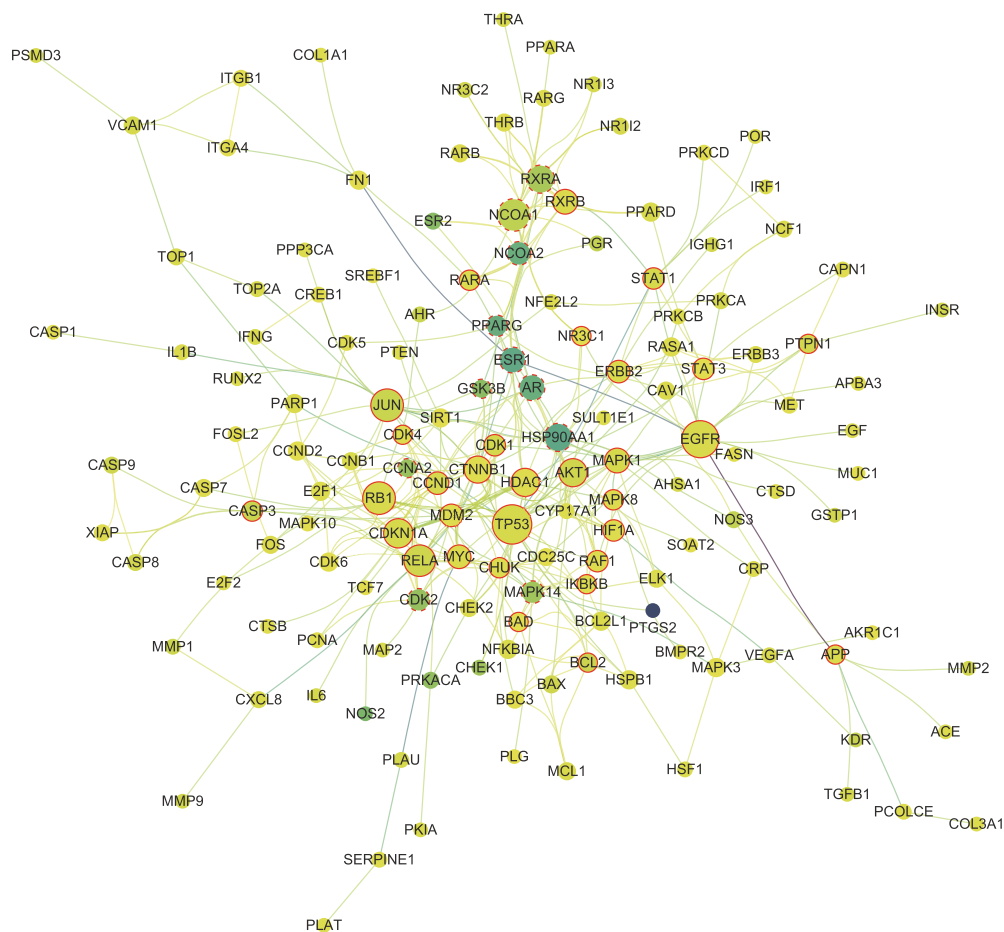


Fig. 3. The protein–protein interaction network showing the 148 predicted RDS targets. The size of each node is proportional to the node degree. The color depth of the node is proportional to the regulated strength score (RSS) of the target. The targets with the highest RSS were heat-shock protein 90 kD α (cytosolic) class A member 1 (HSP90AA1), estrogen receptor 1 (ESR1), androgen receptor (AR), peroxisome proliferator-activated receptor γ (PPARG) and nuclear receptor coactivator 2 (NCOA2). Forty-two hub genes were circled in red line (solid and dotted line) and 11 genes with an RSS >30 were circled in red dotted line. RDS: Respiratory Detox Shot.

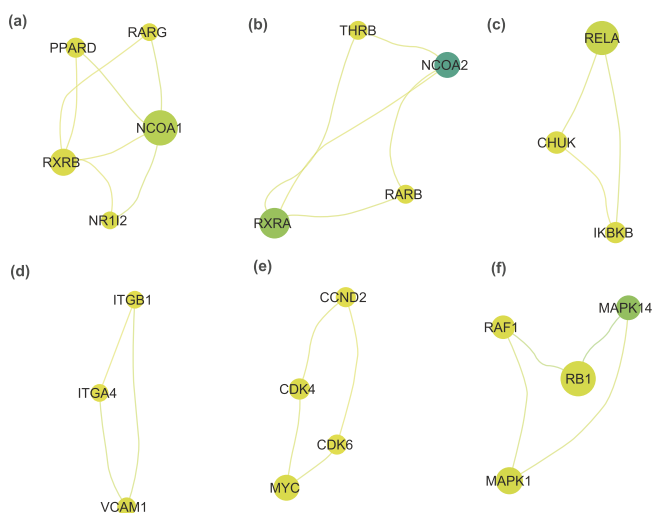


Fig. 4. Cluster analysis and protein-complex recognition of the RDS target network. Cluster analysis was performed on the RDS target network to reveal its highly interconnected regions. Six clusters were identified, indicating their closely related biological functions. RDS: Respiratory Detox Shot.

drugs. Out of the 118 constituents, 48 had molecular binding affinity with 3CL^{pro} that was far less than -5.0 kJ/mol. This indicates that numerous bioactive compounds in RDS have the potential to

interact directly with SARS-CoV-2, in addition to their effects on the body (Fig. 7 and Table 2).

To validate the accuracy and sensitivity of the computational parameters used in the molecular docking, we also tested 14 approved antiviral drugs with reported clinical application against SARS-CoV-2, and the results were consistent with previous studies (Fig. 7 and Table 2).

Based on the network pharmacology and molecular docking analysis, we purchased pure samples of the 48 compounds with modeled binding affinity to perform an *in vitro* 3CL^{pro} inhibition assay, which would help to validate their bioactivity. It was found that at a concentration of 100 μ mol/L, 22 of the candidates had an inhibition rate of greater than 50% (data not shown). The 22 samples with validated 3CL^{pro} inhibition activity were then quantified in the RDS formula using LC–MS analysis of RDS decoction.

3.3. Phytochemical analysis of RDS

Satisfactory separation of major peaks was achieved in both negative and positive ion modes (Fig. 8 and Fig. S3). By comparison with the TCM library, 116 peaks were identified or tentatively characterized by element composition and fragment-matching analyses; these are listed in online supplementary Table S4.

Among them, 47 of the identified constituents may be from *Lonicerae Japonicae* Flos, and 21 may be from *Forsythiae* Fructus, which provided half of the identified constituents. Glycyrrhizae

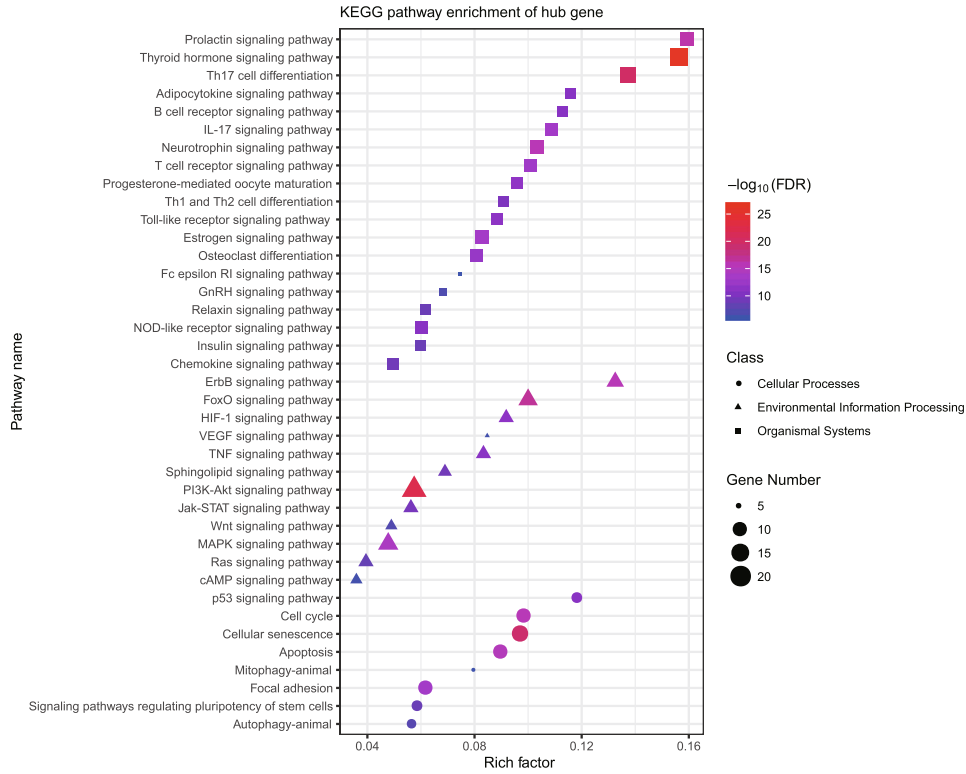


Fig. 5. Kyoto Encyclopedia of Genes and Genomes pathway enrichment of the 42 RDS hub genes. Forty-two hub genes were analyzed for functional enrichment analysis using the STRING database, with FDR set at 1×10^{-6} . A total of 39 pathways were identified and were mainly related to biological functions such as signal transduction, transport and catabolism and cell growth and death. Symbol size is proportional to the number of genes included. FDR: false discovery rate; RDS: Respiratory Detox Shot.

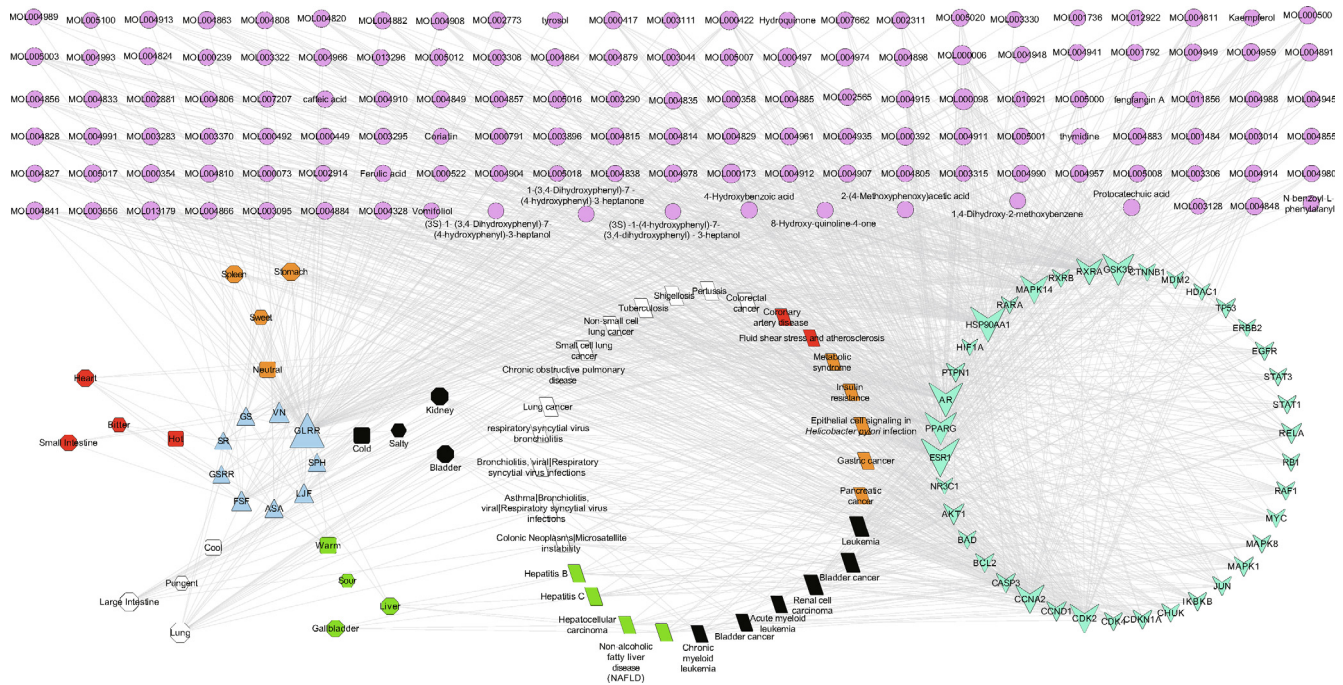


Fig. 6. The intricate network includes the disease pathways, their corresponding meridian tropism, RDS hub genes, the corresponding chemical constituents and traditional Chinese medicine ingredients. The circle in the center described the disease pathways and their corresponding meridian tropism. Nearly half of the disease pathways were related to the Lung meridian (white quadrangles), followed by the Stomach (yellow quadrangles) and Kidney meridians (black quadrangles). They all matched the primary therapeutic effects and the underlying Zang-fu viscera theory of the RDS prescription. ASA: Armeniacae Semen Amarum (Kuxingren); FSF: Forsythiae Fructus (Lianqiao); GLRR: Glycyrrhizae Radix et Rhizoma (Gancao); GS: Gleditsiae Spina (Zaojiaoci); GSRR: Ginseng Radix et Rhizoma (Renshen); LJF: Lonicerae Japonicae Flos (Jinyinhua); RDS: Respiratory Detox Shot; SPH: Schizonepetae Herba (Jingjie); SR: Scrophulariae Radix (Xuanshen); VN: Nidus Vespa (Fengfang).

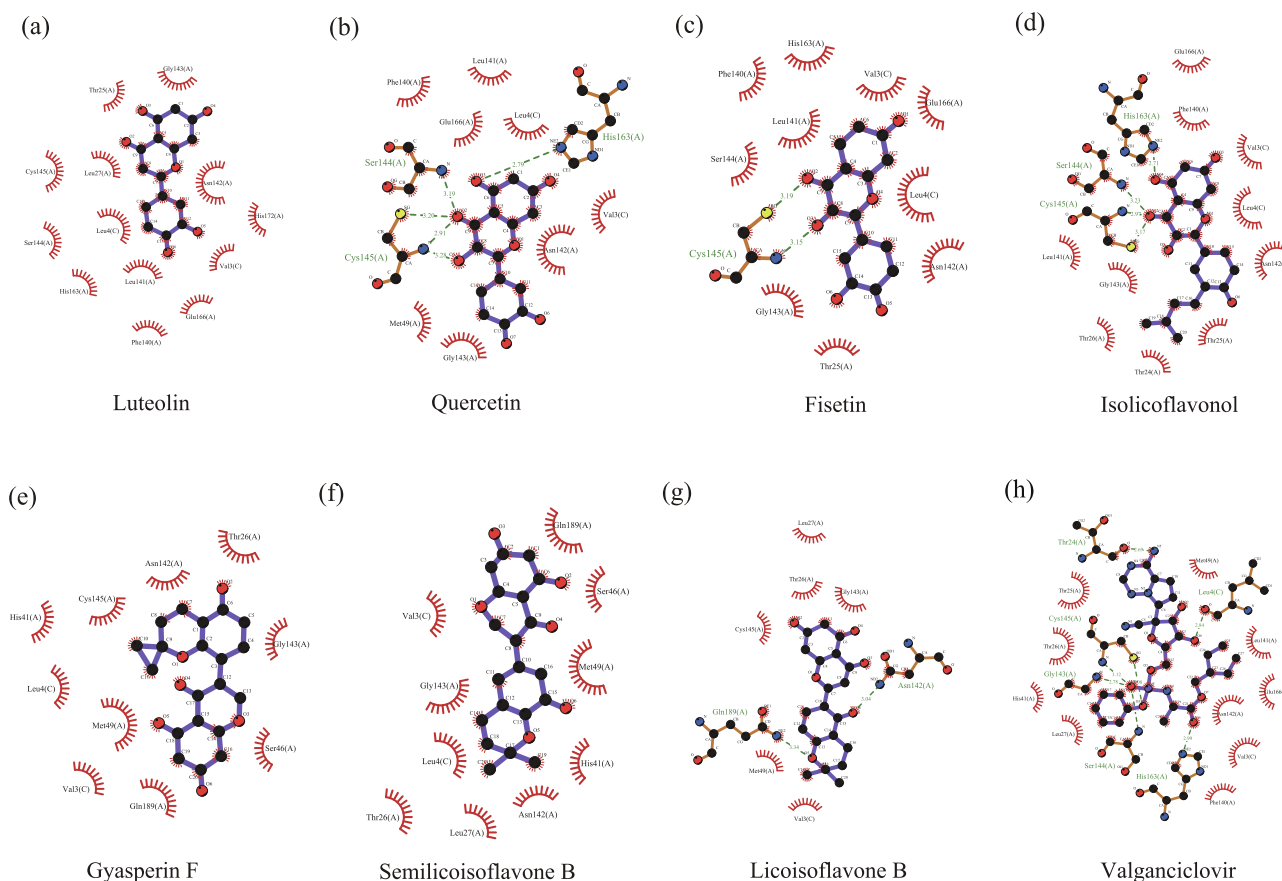


Fig. 7. RDS candidate compounds and representative results of molecular docking with severe acute respiratory syndrome coronavirus 2 3CL^{pro} (6LU7). Schematic diagrams demonstrated the 3CL^{pro} binding sites and proximate affinity of candidate compounds in RDS and valganciclovir, an antiviral drug approved by the US Food and Drug Administration. Black dots: carbon atoms; blue dots: nitrogen atoms; red dots: oxygen atoms; green dotted lines: hydrogen bonds; red combs: amino acid residues. 3CL^{pro}: 3-chymotrypsin-like protease; RDS: Respiratory Detox Shot.

Radix et Rhizoma contained 20 of the constituents, and 16 of them were found in Ginseng Radix et Rhizoma. About 80% of the constituents were provided by 4 herbs. The other 5 herbs contained less than 10 of the identified constituents.

Based on the results from virtual screening and *in vitro* 3CL^{pro} inhibition assay, we performed LC–MS-targeted extraction and analysis of the 22 bioactive constituents in combination with their chemical standards and the sample solution prepared from the water decoction of RDS. In the RDS sample, seven bioactive compounds could be identified and confirmed (Table 3).

4. Discussion

In the current study, the prevention and treatment of the new coronavirus pneumonia with RDS was analyzed systematically. We used a computer-based rational prediction and exploration method to identify candidate chemical constituents from the ingredients of the RDS formula, based on TCM theory and documented patterns of interaction. These candidate chemical constituents were validated using pure samples and their presence in RDS was verified using LS–MS. Intricate networks were constructed for chemical constituents of RDS to unveil the complex interactions among its nine ingredients, properties, flavors and meridian tropisms. Analyzing the treatment principle and method from a systemic perspective, it reveals that RDS achieves its therapeutic effects mainly targeting the Lung and involving other Zang-fu viscera simultaneously.

In the cluster analysis of the RDS network, six submodules were identified, covering 23 out of the 148 targets. Gene ontology analysis of STRING revealed that most genes were related to nucleoplasm, and all six submodules are highly interconnected in their biological functions. Enrichment analysis of protein complex-based gene sets was performed to further reveal the structural and functional connections of the 23 genes in the submodules. The results showed that gene products can form “integrin α 4 β 1: VCAM-1” protein complex (Fig. 4d) and I κ B kinase complex (Fig. 4c). These results indicated that the 23 genes in the submodules may be functionally connected and synergistically regulated. It is well known that VCAM-1 plays an important role in leukocyte migration and inflammatory response, by interacting with integrin α -4/ β -1 (ITGA4/ITGB1) on leukocytes [51,52]. Also, I κ B kinase complex is the master regulator of the canonical nuclear factor κ B inflammation pathway, which is closely related to the body's inflammatory response [53,54]. RDS may have regulatory effects on the formation of an inflammatory storm to reduce excessive inflammation of the body, which ameliorates the severe systemic damage in COVID-19 patients.

The 148 targets in the RDS network were further scrutinized and 42 genes were defined as “hub genes” of the network, which usually have more significant influence and play a more critical role in the network. Forty-two hub genes were identified in the RDS target network (Fig. 3). We introduced the RSS parameter to measure the strength of regulatory effects on hub genes. The higher the RSS score is, the stronger the RDS effect on the hub

Table 2
The binding energy values of the core compounds in RDS and effective drugs reported clinically with SARS-CoV-2 3CL^{pro}.

No.	Source	ID	English name	OB (%)	DL	Molecular formula	Molecular weight (D)	3CL ^{pro} binding affinity (kJ/mol)
0	PDB	Peptide-like/inhibitor	Gluc7_ligand			C ₃₅ H ₄₈ N ₆ O ₈	680.79	-24.70
1	ASA	MOL010921	Estrone	53.56	0.32	C ₁₈ H ₂₂ O ₂	270.16	-23.44
2	ASA	MOL002311	Glycerol	90.78	0.67	C ₂₁ H ₁₈ O ₆	366.11	-24.28
3	ASA	MOL004355	Spinasterol	42.98	0.76	C ₂₉ H ₄₈ O	412.37	-22.60
4	ASA	MOL004841	Licochalcone B	76.76	0.19	C ₁₆ H ₁₄ O ₅	286.08	-22.60
5	ASA	MOL004903	Liquiritin	65.69	0.74	C ₂₁ H ₂₂ O ₉	418.13	-28.88
6	ASA	MOL004908	Glabridin	53.25	0.47	C ₂₀ H ₂₀ O ₄	324.14	-24.70
7	ASA	MOL012922	l-SPD	87.35	0.54	C ₁₉ H ₂₁ NO ₄	327.15	-25.53
8	GSRR	MOL000358	β-sitosterol	36.91	0.75	C ₂₉ H ₅₀ O	414.72	-20.93
9	GSRR	MOL000422	Kaempferol	41.88	0.24	C ₁₅ H ₁₀ O ₆	286.24	-24.70
10	FSF	MOL003283	(2R,3R,4S)-4-(4-hydroxy-3-methoxy-phenyl)-7-methoxy-2,3-dimethylol-tetralin-6-ol	66.51	0.39	C ₂₀ H ₂₄ O ₆	360.41	-24.70
11	FSF	MOL003305	PHILLYRIN	36.40	0.86	C ₂₇ H ₃₄ O ₁₁	534.56	-23.44
12*	FSF	MOL000006	Luteolin	36.16	0.25	C ₁₅ H ₁₀ O ₆	286.24	-28.88
13*	FSF	MOL000098	Quercetin	46.43	0.28	C ₁₅ H ₁₀ O ₇	302.24	-27.21
14*	GS	MOL013179	Fisetin	52.60	0.24	C ₁₅ H ₁₀ O ₆	286.24	-27.21
15	GS	MOL013296	Fustin	50.91	0.24	C ₁₅ H ₁₂ O ₆	288.26	-25.95
16	GS	MOL000449	Stigmasterol	43.83	0.76	C ₂₉ H ₄₈ O	412.70	-23.44
17	SR	MOL002222	Sugiol	36.11	0.28	C ₂₀ H ₂₈ O ₂	300.44	-24.28
18	SR	MOL007662	Harpagoside _{qt}	122.87	0.32	C ₁₈ H ₂₀ O ₆	332.35	-23.86
19	SPH	MOL011856	Schkuhriin I	54.45	0.52	C ₂₂ H ₂₈ O ₈	420.18	-27.21
20	SPH	MOL002881	Diosmetin	31.14	0.27	C ₁₆ H ₁₂ O ₆	300.06	-23.86
21	VN		Coriatin	Good	Accepted	C ₁₅ H ₁₈ O ₅	278.12	-24.28
22	GLRR	MOL004898	(E)-3-[3,4-dihydroxy-5-(3-methylbut-2-enyl)phenyl]-1-(2,4-dihydroxyphenyl)prop-2-en-1-one	46.27	0.31	C ₂₀ H ₂₀ O ₅	340.38	-23.44
23	GLRR	MOL004904	Licopyranocoumarin	80.36	0.65	C ₂₁ H ₂₀ O ₇	384.38	-25.12
24	GLRR	MOL004910	Glabranin	52.90	0.31	C ₂₀ H ₂₀ O ₄	324.38	-24.70
25	GLRR	MOL004911	Glabrene	46.27	0.44	C ₂₀ H ₁₈ O ₄	322.36	-28.46
26	GLRR	MOL004912	Glabrone	52.51	0.50	C ₂₀ H ₁₆ O ₅	336.34	-28.05
27	GLRR	MOL004915	Eurycarpin A	43.28	0.37	C ₂₀ H ₁₈ O ₅	338.36	-24.28
28*	GLRR	MOL004949	Isolicoflavonol	45.17	0.42	C ₂₀ H ₁₈ O ₆	354.36	-26.37
29	GLRR	MOL004959	1-Methoxyphaseollidin	69.98	0.64	C ₂₁ H ₂₂ O ₅	354.40	-23.86
30	GLRR	MOL004961	Quercetin der.	46.45	0.33	C ₁₇ H ₁₄ O ₇	330.29	-26.79
31	GLRR	MOL000497	Licochalcone A	40.79	0.29	C ₂₁ H ₂₂ O ₄	338.40	-22.60
32	GLRR	MOL000500	Vestitol	74.66	0.21	C ₁₆ H ₁₆ O ₄	272.30	-24.28
33	GLRR	MOL005008	Glycyrrhiza flavonol A	41.28	0.60	C ₂₀ H ₁₈ O ₇	370.36	-25.53
34	GLRR	MOL001484	Inermine	75.18	0.54	C ₁₆ H ₁₂ O ₅	284.27	-23.86
35	GLRR	MOL000239	Jaranol	50.83	0.29	C ₁₇ H ₁₄ O ₆	314.29	-24.28
36	GLRR	MOL000354	Isorhamnetin	49.60	0.31	C ₁₆ H ₁₂ O ₇	316.27	-25.12
37	GLRR	MOL003656	Lupiwighteone	51.64	0.37	C ₂₀ H ₁₈ O ₅	338.36	-23.86
38	GLRR	MOL000392	Furmononetin	69.67	0.21	C ₁₆ H ₁₂ O ₄	268.27	-25.12
39	GLRR	MOL000417	Calycosin	47.75	0.24	C ₁₆ H ₁₂ O ₅	284.27	-25.12
40	GLRR	MOL004328	Naringenin	59.29	0.21	C ₁₅ H ₁₂ O ₅	272.26	-24.28
41*	GLRR	MOL004810	Glyasperin F	75.84	0.54	C ₂₀ H ₁₈ O ₆	354.36	-27.21
42	GLRR	MOL004811	Glyasperin C	45.56	0.40	C ₂₁ H ₂₄ O ₅	356.42	-24.28
43*	GLRR	MOL004827	Semilicoisoflavone B	48.78	0.55	C ₂₀ H ₁₆ O ₆	352.34	-25.53
44	GLRR	MOL004829	Glepidotin B	64.46	0.34	C ₂₀ H ₂₀ O ₅	340.38	-26.37
45	GLRR	MOL004856	Gancaonin A	51.08	0.40	C ₂₁ H ₂₀ O ₅	352.39	-24.28
46	GLRR	MOL004879	Glycyrin	52.61	0.47	C ₂₂ H ₂₂ O ₆	382.41	-24.28
47*	GLRR	MOL004884	Licoisoflavone B	38.93	0.55	C ₂₀ H ₁₆ O ₆	352.34	-26.79
48	GLRR	MOL004885	Licoisoflavanone	52.47	0.54	C ₂₀ H ₁₈ O ₆	354.36	-24.28
s1			Lopinavir			C ₃₇ H ₄₈ N ₄ O ₅	628.80	-22.19
s2			Ritonavir			C ₃₇ H ₄₈ N ₆ O ₅ S ₂	720.96	-24.28
s3			Remdesivir			C ₂₇ H ₃₅ N ₆ O ₈ P	602.58	-28.05
s4			Darunavir			C ₂₇ H ₃₇ N ₃ O ₇ S	547.66	-24.28
s5			Arbidol			C ₂₂ H ₂₅ BrN ₂ O ₃ S	531.89	-21.35
s6			Chloroquine			C ₁₈ H ₂₆ ClN ₃	319.87	-18.84
s7			Indinavir			C ₃₆ H ₄₇ N ₅ O ₄	613.79	-26.79
s8			Saquinavir			C ₃₈ H ₅₀ N ₆ O ₅	670.84	-30.56
s9			Nelfinavir			C ₃₂ H ₄₅ N ₃ O ₄ S	567.78	-25.53
s10			Tipranavir			C ₃₁ H ₃₃ F ₃ N ₂ O ₅ S	602.66	-27.63
s11			Cyclosporin A			C ₆₂ H ₁₁₁ N ₁₁ O ₁₂	1202.64	171.62
s12			Vancomycin			C ₆₆ H ₇₅ Cl ₂ N ₉ O ₂₄	1449.25	114.69
s13			Ribavirin			C ₈ H ₁₂ N ₄ O ₅	244.20	-25.95
s14			Valganciclovir			C ₁₄ H ₂₂ N ₆ O ₅	354.36	-26.79

RDS core compounds and their binding affinity with 3CL^{pro} were presented. *: compounds identified and confirmed in the following liquid chromatography-tandem mass spectrometry analysis. ASA: Armeniaceae Semen Amarum (Kuxingren); 3CL^{pro}: 3-chymotrypsin-like protease; D: Daltons; DL: drug-likeness; FSF: Forsythiae Fructus (Lian-qiao); GLRR: Glycyrrhizae Radix Et Rhizoma (Gancao); GS: Gleditsiae Spina (Zaojiaoci); GSRR: Ginseng Radix Et Rhizoma (Ren Shen); LJF: Lonicerae Japonicae Flos (Jinyinhua); PDB: protein data bank; OB: oral bioavailability; RDS: Respiratory Detox Shot; SARS-CoV-2: severe acute respiratory syndrome coronavirus 2; SPH: Schizonepetae Herba (Jingjie); SR: Scrophulariae Radix (Xuanshen); VN: Vespaee Nidus (Fengfang).

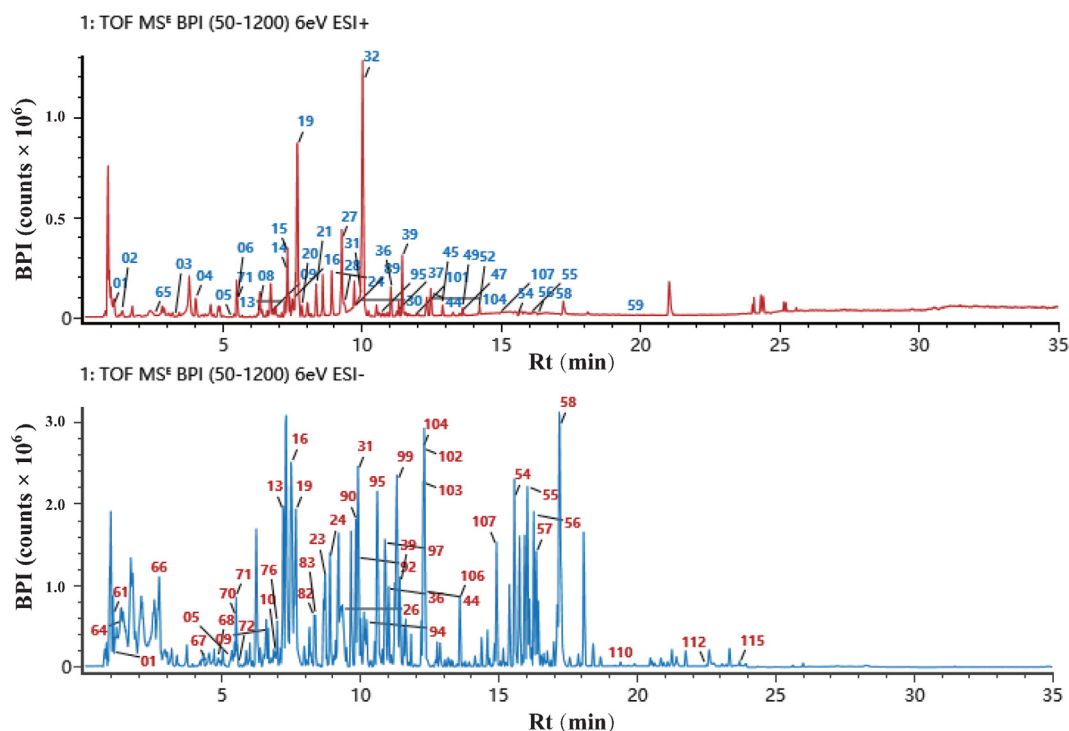


Fig. 8. Representative base ion chromatograms of Respiratory Detox Shot from the ultra high-performance liquid chromatography/quadrupole time-of-flight mass spectrometry analysis. Base ion chromatograms of the positive ions (upper) and the negative ions (lower) were obtained for candidate compounds. The X-axis represents retention time (minutes) of the chromatogram. The Y-axis represents intensity (counts) of peaks in the chromatogram. BPI: base peak intensity; Rt: retention time.

Table 3
Screen targeted compounds in total ion chromatogram of liquid chromatography mass spectrometry.

No.	Compound	Origin	Rt (min)	Adduct	Mass-to-charge ratio (m/z)	Mass error ($\times 10^{-6}$)	Formula	Name
1	C020*	<i>Forsythiae Fructus</i>	13.49	+H/-H	287.0541/285.0401	-3.1/-1.3	C ₁₅ H ₁₀ O ₆	Luteolin
2	C116*	<i>Glycyrrhizae Radix et Rhizoma</i>	22.66	-H	351.0868	-1.6	C ₂₀ H ₁₆ O ₆	Licoisoflavone B
3	C023*	<i>Gleditsiae Spina</i>	13.49	+H/-H	287.0541/285.0401	-3.1/-1.3	C ₁₅ H ₁₀ O ₆	Fisetin
4	C022*	<i>Forsythiae Fructus</i>	9.84	+H	303.0493	-2.2	C ₁₅ H ₁₀ O ₇	Quercetin
5	C093*	<i>Glycyrrhizae Radix et Rhizoma</i>	20.69	-H	353.1021	-2.9	C ₂₀ H ₁₈ O ₆	Glyasperin F
6	C057*	<i>Glycyrrhizae Radix et Rhizoma</i>	20.09	+H	355.1175	-0.3	C ₂₀ H ₁₈ O ₆	Isolicoflavonol
7	C099*	<i>Glycyrrhizae Radix et Rhizoma</i>	22.66	-H	351.0868	-1.6	C ₂₀ H ₁₆ O ₆	Semilicoisoflavone-B

* The peak in chromatogram of sample solution had the same retention time in chromatogram of standard solution. Rt: retention time.

genes. There are 11 genes most strongly affected by the compounds in RDS. Thus, these 11 genes may play a more significant role in therapeutic effects of RDS prescription.

From the 42 hub genes, 39 pathways were identified from the pathway enrichment analysis, and the most important were signal transduction, transport and catabolism, cell growth and death, cellular community-eukaryotes, immune system, neural system, nervous system, development and regeneration (Fig. 5). This result indicated that these pathways might be critical biological processes through which RDS achieves its therapeutic effect.

The enrichment analysis of 42 hub genes with STRING and DAVID databases identified disease pathways that involved 38 targets related to 134 chemical constituents of the nine ingredients of RDS (Fig. 6). These results demonstrated the complex regulatory mechanism of TCM, which involves multiple bioactive constituents working on multiple targets and acting on multiple disease pathways. Importantly, viral infection-related pathways were also indicated in the disease pathway enrichment analysis (Fig. S2), indicating potential therapeutic effects of RDS on viral infections.

Based on the “disease-targets-constituents” network, the five most connected genes were *ESR1*, *HSP90AA1*, *AR*, *PPARG* and *GSK3B*;

this result agreed with the protein-protein interaction analysis shown in Fig. 3. All five genes were in key nodes of the RDS network, indicating that these compounds and targets may play a greater regulatory function in the RDS network. Delving further into the biological functions of the five genes and their proteins, all have significant roles in gene expression, cellular proliferation and differentiation, while *PPARG* and *GSK3B* are also involved in lipid and glucose metabolism, respectively. RDS may affect these crucial host cellular pathways to enhance overall health of the body and improve the body's ability to fight against viruses. Unlike SARS, where the most affected organ is the lung, the new coronavirus attacks not only the lung, but also the heart, kidneys, intestines and other organs, causing multiple organ failure within a short time window. Although the disease is located in the lung and requires immediate medical care, in TCM theory it is necessary to consider that deficiency of the Lung will affect the Stomach and the Spleen and damage the Heart and the Kidneys as well. Based on the analysis of the ingredients and meridian tropism network, seven out of nine ingredients enter the Lung meridian, because the disease is located in the Lungs and should be treated with priority. Through the present analysis, which incorporates elements

of allopathic medicine and TCM meridian tropism, it can be seen that TCM encompasses therapeutic effects that may extend beyond our current scientific, measurable understanding of the disease process. Fortunately, the lack of precision in pairing TCM's theoretical framework with the currently-known understanding of COVID-19 has not hindered its successful application in this critical disease. The RDS formula focuses on, and often successfully treats, the body as a whole, rather than treating isolated symptoms.

The present network analysis used an integrative perspective to explore connections and interactions among the chemical constituents of the RDS formula, their targets and pathways, as well as how the bioactive components of RDS may work on the human body to combat COVID-19. However, it is unknown whether the candidate compounds in RDS have any anti-coronavirus activity, such as blocking the penetration, uncoating or synthesis of viral proteins or nucleic acids. The SARS-CoV-2 3CL^{pro} (PDB: 6LU7) is required for the replication of coronaviruses and considered a validated target in the design of potential anti-coronavirus inhibitors [20,22,23]. A computational strategy for modeling molecular docking was used to evaluate the affinity between candidate constituents of RDS and 3CL^{pro}. This technique helps to identify RDS constituents that may interact directly with SARS-CoV2 (Fig. 7). After preliminary screening, 48 constituents demonstrated binding affinity with 3CL^{pro}; using commercially available samples of these constituents, 22 out of the 48 had inhibition rates greater than 50% at a concentration of 100 μmol/L, in the 3CL^{pro} inhibition assay (unpublished data). These results indicate that the bioactive constituents of RDS might possess direct anti-SARS-CoV-2 activity in addition to their effects on the body. In the phytochemical analysis of RDS, about 80% of the constituents identified were provided by four of the nine herbs in the formula. The other five herbs each contained fewer than 10 of the identified constituents. Based on the results from the virtual screening and the *in vitro* 3CL^{pro} inhibition assay, seven out of 22 bioactive constituents could be identified and confirmed using LC–MS targeted extraction and analysis (Table 3). The results suggested that these seven bioactive compounds could be used in a subsequent study for drug discovery and could be important makers for quality control testing of the prescription.

A literature search was also performed to retrieve prior studies on the seven bioactive compounds identified in this study [13]. Half of the ingredients in the RDS prescription are classic toxin-clearing TCM with antiviral activity, including Forsythiae Fructus, Lonicerae Japonicae Flos, Schizonepetae Herba, Gleditsiae Spina and Nidus Vespae [11]. Among the seven compounds, luteolin [55–58] and quercetin [59] from Forsythiae Fructus, and fisetin from Gleditsiae Spina [60] have been studied for their toxin-clearing and antiviral activities. Besides, some understudied compounds from Glycyrrhizae Radix et Rhizoma (e.g., licoisoflavone B, glyasperin F, isolicoisoflavonol and semilicoisoflavone-B) have also shown similar inhibitory effects against 3CL^{pro}, indicating their antiviral potential. These bioactive constituents and ingredients should be considered to be new candidate drugs and may provide novel perspectives to antiviral drug discovery and development.

5. Conclusions

Inspired by the fact that the TCM prescription, Lung-toxin Dispelling Formula No. 1 (RDS), has been successfully used clinically to treat severe and critical cases of COVID-19 in China, and has been used as a preventive dietary supplement for COVID-19 in the US, this study applied network pharmacology, molecular docking and UPLC/QTOF MS approaches to reveal the complex interactions between the TCM prescription and the disease. In this study, the multi-faceted system of TCM prescription has been integrated

with the targets, disease pathways and their Zang-fu viscera to show an intricate network of interaction. This work shows that applying modern biological and pharmacological technologies to TCM research can deepen the mechanistic understanding of TCM compound formulas and better promote their clinical application. There is no doubt that the establishment of novel prescriptions based on TCM theory requires more effective integration of sub-disciplines and technologies.

To further understand the underlying mechanisms of TCM, future studies will analyze the biochemically active compounds present in RDS and their mechanisms of action, using metabolomics, proteomics and other state of the art technologies.

Funding

We are grateful for the financial support from National Key Research and Development Program of China (No. 2018YFC1707900).

Author contribution

Conceptualization, Wu Wa., Hofmann L.A., and Ci Z.; methodology, Wu We., Hou J., Zhang L., Li F., Gao L., Wu X., Shi J., Zhang R., Long H. and Lei M.; software, Wu We., Hou J. and Zhang L.; validation, Zhang Z., Hou J. and Lei M.; writing—original draft preparation, Zhang Z., Wu Wa., Wu We. and Hou J.; writing—review and editing, Wu Wa., Zhang Z., Guo D., Chen K., Hofmann L.A. and Ci Z.; All authors have read and agreed to the published version of the manuscript.

Conflicts of interest

The authors declare that there is no conflict of interest.

Appendix A. supplementary data

Supplementary data to this article can be found online at <https://doi.org/10.1016/j.joim.2020.03.004>.

References

- [1] Regional Office for Europe, World Health Organization. 2019-nCoV outbreak is an emergency of international concern. (2020-01-31) [2020-03-04]. <http://www.euro.who.int/en/health-topics/health-emergencies/international-health-regulations/news/news/2020/2/2019-ncov-outbreak-is-an-emergency-of-international-concern>.
- [2] Al-Mandhari A, Samhouri D, Abubakar A, Brennan R. Coronavirus disease 2019 outbreak: preparedness and readiness of countries in the Eastern Mediterranean Region. *East Mediterr Health J* 2020;26(2):136–7.
- [3] Song P, Karako T. COVID-19: real-time dissemination of scientific information to fight a public health emergency of international concern. *Biosci Trends* 2020;14(1):1–2.
- [4] World Health Organization. WHO statement on cases of COVID-19 surpassing 100 000. (2020-03-37) [2020-03-18]. <https://www.who.int/news-room/detail/07-03-2020-who-statement-on-cases-of-covid-19-surpassing-100-000>.
- [5] Wilder-Smith A, Chiew CJ, Lee VJ. Can we contain the COVID-19 outbreak with the same measures as for SARS?. *Lancet Infect Dis* 2020. [https://doi.org/10.1016/S1473-3099\(20\)30129-8](https://doi.org/10.1016/S1473-3099(20)30129-8).
- [6] Xiao Y, Torok ME. Taking the right measures to control COVID-19. *Lancet Infect Dis* 2020. [https://doi.org/10.1016/S1473-3099\(20\)30152-3](https://doi.org/10.1016/S1473-3099(20)30152-3).
- [7] Ren JL, Zhang AH, Wang XJ. Traditional Chinese medicine for COVID-19 treatment. *Pharmacol Res* 2020;155:104743.
- [8] Luo H, Tang QL, Shang YX, Liang SB, Yang M, Robinson N, et al. Can Chinese medicine be used for prevention of corona virus disease 2019 (COVID-19)? A review of historical classics, research evidence and current prevention programs. *Chin J Integr Med* 2020;26(4):243–50.
- [9] Wang Z, Chen X, Lu Y, Chen F, Zhang W. Clinical characteristics and therapeutic procedure for four cases with 2019 novel coronavirus pneumonia receiving combined Chinese and Western medicine treatment. *Biosci Trends* 2020;14(1):64–8.
- [10] Li SY, Li GY, Zhang HR, Li B, Hofmann HA, Ci ZH. Clinical efficacy and experiences of Lung-toxin Dispelling Formula No.1 treating patients of corona

- virus disease 2019 type severe/type extremely severe. *Zhongguo Shi Yan Fang Ji Xue Za Zhi* 2020;26(11). <https://doi.org/10.13422/j.cnki.syfxjx.20200843> [Chinese with abstract in English].
- [11] Ling CQ. Traditional Chinese medicine is a resource for drug discovery against 2019 novel coronavirus (SARS-CoV-2). *J Integr Med* 2020;18(2):87–8.
 - [12] Xu K, Cai H, Shen Y, Ni Q, Chen Y, Hu S, et al. Management of corona virus disease-19 (COVID-19): the Zhejiang experience. *Zhejiang Da Xue Xue Bao Yi Xue Ban* 2020;49(1). <https://doi.org/10.3785/j.issn.1008-9292.2020.02.02> [Chinese with abstract in English].
 - [13] Zhang DH, Wu KL, Zhang X, Deng SQ, Peng B. *In silico* screening of Chinese herbal medicines with the potential to directly inhibit 2019 novel coronavirus. *J Integr Med* 2020;18(2):152–8.
 - [14] Li S. Exploring traditional Chinese medicine by a novel therapeutic concept of network target. *Chin J Integr Med* 2016;22(9):647–52.
 - [15] Luo TT, Lu Y, Yan SK, Xiao X, Rong XL, Guo J. Network pharmacology in research of Chinese medicine formula: methodology, application and prospective. *Chin J Integr Med* 2020;26(1):72–80.
 - [16] Boezio B, Audouze K, Ducrot P, Taboureau O. Network-based approaches in pharmacology. *Mol Inform* 2017;36(10). <https://doi.org/10.1002/minf.201700048>.
 - [17] Berger SI, Iyengar R. Network analyses in systems pharmacology. *Bioinformatics* 2009;25(19):2466–72.
 - [18] Li S, Zhang B. Traditional Chinese medicine network pharmacology: theory, methodology and application. *Chin J Integr Med* 2013;11(2):110–20.
 - [19] Wu W, Zhang Z, Li F, Deng Y, Lei M, Long H, et al. A network-based approach to explore the mechanisms of *Uncaria* alkaloids in treating hypertension and alleviating Alzheimer's disease. *Int J Mol Sci* 2020;21(5). <https://doi.org/10.3390/ijms21051766>.
 - [20] Xiong B, Gui CS, Xu XY, Luo C, Chen J, Luo HB, et al. A 3D model of SARS-CoV 3CL proteinase and its inhibitors design by virtual screening. *Acta Pharmacol Sin* 2003;24(6):497–504.
 - [21] Ratia K, Saikatendu KS, Santarsiero BD, Barretto N, Baker SC, Stevens RC, et al. Severe acute respiratory syndrome coronavirus papain-like protease: structure of a viral deubiquitinating enzyme. *Proc Natl Acad Sci U S A* 2006;103(15):5717–22.
 - [22] Wu C, Liu Y, Yang Y, Zhang P, Zhong W, Wang Y, et al. Analysis of therapeutic targets for SARS-CoV-2 and discovery of potential drugs by computational methods. *Acta Pharm Sin B* 2020. <https://doi.org/10.1016/j.apsb.2020.02.008>.
 - [23] Theerawatanasirikul S, Kuo CJ, Phetcharat N, Lekcharoensuk P. *In silico* and *in vitro* analysis of small molecules and natural compounds targeting the 3CL protease of feline infectious peritonitis virus. *Antiviral Res* 2020;174:104697.
 - [24] Mukherjee P, Shah F, Desai P, Avery M. Inhibitors of SARS-3CL^{pro}: virtual screening, biological evaluation, and molecular dynamics simulation studies. *J Chem Inf Model* 2011;51(6):1376–92.
 - [25] Morse JS, Lalonde T, Xu S, Liu WR. Learning from the past: possible urgent prevention and treatment options for severe acute respiratory infections caused by 2019-nCoV. *ChemBioChem* 2020;21(5):730–8.
 - [26] Yates B, Braschi B, Gray KA, Seal RL, Tweedie S, Bruford EA. Genenames.org: the HGNC and VGNC resources in 2017. *Nucleic Acids Res* 2017;45(D1):D619–25.
 - [27] Xu HY, Zhang YQ, Liu ZM, Chen T, Lv CY, Tang SH, et al. ETCM: an encyclopaedia of traditional Chinese medicine. *Nucleic Acids Res* 2019;47(D1):D976–82.
 - [28] Wu Y, Zhang F, Yang K, Fang S, Bu D, Li H, et al. SymMap: an integrative database of traditional Chinese medicine enhanced by symptom mapping. *Nucleic Acids Res* 2019;47(D1):D1110–7.
 - [29] Zeng X, Zhang P, He W, Qin C, Chen S, Tao L, et al. NPASS: natural product activity and species source database for natural product research, discovery and tool development. *Nucleic Acids Res* 2018;46(D1):D12170–222.
 - [30] Xue R, Fang Z, Zhang M, Yi Z, Wen C, Shi T. TCMID: Traditional Chinese medicine integrative database for herb molecular mechanism analysis. *Nucleic Acids Res* 2013;41(Database issue):D1089–95.
 - [31] Ru J, Li P, Wang J, Zhou W, Li B, Huang C, et al. TCMSPP: a database of systems pharmacology for drug discovery from herbal medicines. *J Cheminform* 2014;6(1):13.
 - [32] Pharmacopoeia NCOC. Pharmacopoeia of People's Republic of China, Vol. 1. Beijing: China Medical Science Press; 2015.
 - [33] Shannon P, Markiel A, Ozier O, Baliga NS, Wang JT, Ramage D, et al. Cytoscape: a software environment for integrated models of biomolecular interaction networks. *Genome Res* 2003;13(11):2498–504.
 - [34] Lagorce D, Bouslama L, Becot J, Miteva MA, Villoutreix BO. FAF-Drugs₄: free ADME-tox filtering computations for chemical biology and early stages drug discovery. *Bioinformatics* 2017;33(22):3658–60.
 - [35] Daina A, Michielin O, Zoete V. SwissTargetPrediction: updated data and new features for efficient prediction of protein targets of small molecules. *Nucleic Acids Res* 2019;47(W1):W357–64.
 - [36] Keiser MJ, Roth BL, Armbruster BN, Ernberger P, Irwin JJ, Shoichet BK. Relating protein pharmacology by ligand chemistry. *Nat Biotechnol* 2007;25(2):197–206.
 - [37] Yao ZJ, Dong J, Che YJ, Zhu MF, Wen M, Wang NN, et al. TargetNet: a web service for predicting potential drug-target interaction profiling via multi-target SAR models. *J Comput Aided Mol Des* 2016;30(5):413–24.
 - [38] Uniprot C. UniProt: a worldwide hub of protein knowledge. *Nucleic Acids Res* 2019;47(D1):D506–15.
 - [39] Stelzer G, Rosen N, Plaschkes I, Zimmerman S, Twik M, Fishilevich S, et al. The GeneCards suite: from gene data mining to disease genome sequence analyses. *Curr Protoc Bioinf* 2016;54:1.30–3.
 - [40] Szklarczyk D, Gable AL, Lyon D, Junge A, Wyder S, Huerta-Cepas J, et al. STRING v11: protein-protein association networks with increased coverage, supporting functional discovery in genome-wide experimental datasets. *Nucleic Acids Res* 2019;47(D1):D607–13.
 - [41] Das J, Yu H. HINT: High-quality protein interactomes and their applications in understanding human disease. *BMC Syst Biol* 2012;6(1):92.
 - [42] Zhao J, Tian SS, Yang JJ, Liu JF, Zhang WD. Investigating the mechanism of Qing-Fei-Pai-Du-Tang for treatment of novel coronavirus pneumonia by network pharmacology. *Zhong Cao Yao* 2020;51(4):829–35. [Chinese with abstract in English].
 - [43] Bader GD, Hogue CWV. An automated method for finding molecular complexes in large protein interaction networks. *BMC Bioinf* 2003;4:2.
 - [44] Kamburov A, Stelzl U, Lehrach H, Herwig R. The ConsensusPathDB interaction database: 2013 update. *Nucleic Acids Res* 2013;41(Database issue):D793–800.
 - [45] Kamburov A, Wierling C, Lehrach H, Herwig R. ConsensusPathDB—a database for integrating human functional interaction networks. *Nucleic Acids Res* 2009;37(Database issue):D623–8.
 - [46] Huang DW, Sherman BT, Lempicki RA. Systematic and integrative analysis of large gene lists using DAVID bioinformatics resources. *Nat Protoc* 2009;4(1):44–57.
 - [47] Rose AS, Bradley AR, Valasatava Y, Duarte JM, Prlic A, Rose PW. NGL viewer: web-based molecular graphics for large complexes. *Bioinformatics* 2018;34(21):3755–8.
 - [48] Liu X, Zhang B, Jin Z, Yang H, Rao Z. The crystal structure of COVID-19 main protease in complex with an inhibitor N3. (2020) [2020-03-04]. <https://www.rcsb.org/structure/6lu7>. doi: 10.2210/pdb6LU7/pdb.
 - [49] Morris GM, Huey R, Lindstrom W, Sanner MF, Belew RK, Goodsell DS, et al. AutoDock₄ and AutoDockTools₄: automated docking with selective receptor flexibility. *J Comput Chem* 2009;30(16):2785–91.
 - [50] Trott O, Olson AJ. AutoDock Vina: improving the speed and accuracy of docking with a new scoring function, efficient optimization, and multithreading. *J Comput Chem* 2010;31(2):455–61.
 - [51] Osborn L, Hession C, Tizard R, Vassallo C, Luhowskyj S, Chi-Rosso G, et al. Direct expression cloning of vascular cell adhesion molecule 1, a cytokine-induced endothelial protein that binds to lymphocytes. *Cell* 1989;59(6):1203–11.
 - [52] Yusuf-Makagiansar H, Anderson ME, Yakovleva TV, Murray JS, Siahhan TJ. Inhibition of LFA-1/ICAM-1 and VLA-4/VCAM-1 as a therapeutic approach to inflammation and autoimmune diseases. *Med Res Rev* 2002;22(2):146–67.
 - [53] Solt LA, May MJ. The IκB kinase complex: master regulator of NF-κB signaling. *Immunol Res* 2008;42(1–3):3–18.
 - [54] Karin M. How NF-κB is activated: the role of the IκB kinase (IKK) complex. *Oncogene* 1999;18(49):6867–74.
 - [55] Wu CC, Fang CY, Hsu HY, Chen YJ, Chou SP, Huang SY, et al. Luteolin inhibits Epstein-Barr virus lytic reactivation by repressing the promoter activities of immediate-early genes. *Antiviral Res* 2016;132:99–110.
 - [56] Peng M, Watanabe S, Chan KWK, He Q, Zhao Y, Zhang Z, et al. Luteolin restricts dengue virus replication through inhibition of the proprotein convertase furin. *Antiviral Res* 2017;143:176–85.
 - [57] Peng M, Swarbrick CMD, Chan KW, Luo D, Zhang W, Lai X, et al. Luteolin escape mutants of dengue virus map to prM and NS2B and reveal viral plasticity during maturation. *Antiviral Res* 2018;154:87–96.
 - [58] Yan H, Ma L, Wang H, Wu S, Huang H, Gu Z, et al. Luteolin decreases the yield of influenza A virus *in vitro* by interfering with the coat protein I complex expression. *J Nat Med* 2019;73(3):487–96.
 - [59] Wu W, Li R, Li X, He J, Jiang S, Liu S, et al. Quercetin as an antiviral agent inhibits influenza A virus (IAV) entry. *Viruses* 2015;8(1):6.
 - [60] Li R, Liang HY, Li MY, Lin CY, Shi MJ, Zhang XJ. Interference of fisetin with targets of the nuclear factor-κB signal transduction pathway activated by Epstein-Barr virus encoded latent membrane protein 1. *Asian Pac J Cancer Prev* 2014;15(22):9835–9.